Intracellular neutralization of viral infection in polarized epithelial cells by neonatal Fc receptor (FcRn)-mediated IgG transport

Yu Bai[a,b,1], Lilin Ye[a,1], Devin B. Tesar[c], Haichen Song[d], Deming Zhao[b], Pamela J. Björkman[c,2], Derry C. Roopenian[e], and Xiaoping Zhu[a,2]

[a]Laboratory of Immunology, Virginia–Maryland Regional College of Veterinary Medicine, and Maryland Pathogen Research Institute, University of Maryland, College Park, MD 20742; [b]College of Veterinary Medicine, China Agricultural University, Beijing 100193, China; [c]Division of Biology, The Howard Hughes Medical Institute, California Institute of Technology, Pasadena, CA 91125; [d]Synbiotics, College Park, MD 20742; and [e]Jackson Laboratory, Bar Harbor, ME 04609

Edited by Robert A. Lamb, Northwestern University, Evanston, IL, and approved October 6, 2011 (received for review September 29, 2011)

IgG was traditionally thought to neutralize virions by blocking their attachment to or penetration into mucosal epithelial cells, a common site of exposure to viruses. However, we describe an intracellular neutralizing action for an influenza hemagglutinin-specific monoclonal antibody, Y8-10C2 (Y8), which has neutralizing activity only at an acidic pH. When Y8 was applied to the basolateral surface of Madin–Darby canine kidney cells expressing the rat neonatal Fc receptor for IgG (FcRn), it significantly reduced viral replication following apical exposure of the cell monolayer to influenza virus. Virus neutralization by Y8 mAb was dependent on FcRn expression and its transport of IgG. As both FcRn and Y8 mAb bind their partners only at acidic pH, the Y8 mAb is proposed to carry out its antiviral activity intracellularly. Furthermore, the virus, Y8 mAb, and FcRn colocalized within endosomes, possibly inhibiting the fusion of viral envelopes with endosomal membranes during primary uncoating, and preventing the accumulation of the neutralized viral nucleoprotein antigen in the nucleus. Prophylactic administration of Y8 mAb before viral challenge in WT mice, but not FcRn-KO mice, conferred protection from lethality, prevented weight loss, resulted in a significant reduction in pulmonary virus titers, and largely reduced virus-induced lung pathology. Thus, this study reveals an intracellular mechanism for viral neutralization in polarized epithelial cells that is dependent on FcRn-mediated transport of neutralizing IgG.

The neonatal Fc receptor, FcRn, plays a central role in IgG biology at all stages of life. It is the only known Fc receptor able to transport IgG across cell barriers. At the perinatal stage, FcRn confers the newborn with humoral immunity by transporting maternal IgG across placental and/or neonatal intestinal epithelial cells (reviewed in refs. 1–3). By transcytosing IgG across the vascular endothelium at all stages of life, FcRn ensures the extravascular bioavailability of IgG (1). Finally, by transcytosing IgG across the mucosal epithelium, FcRn provides a line of humoral defense at the mucosal surfaces (3).

In addition to its transcytotic function, FcRn plays a critical role in serum IgG homeostasis by recycling IgG away from a catabolic pathway in vascular endothelium, thus extending its lifespan in circulation and ensuring long-lasting protective immunity after infection (1, 2). A hallmark of FcRn is that it binds IgG at acidic pH ($\leq$6.5) and releases IgG at neutral or higher pH (4). In the majority of cell types, FcRn resides primarily in early acidic endosomal vesicles (5, 6); FcRn binds to IgG that enters the cell by pinocytosis or endocytosis. Subsequently, FcRn efficiently recycles IgG back to the plasma membrane or transcytoses it to the opposite plasma membrane, where the near-neutral pH of the extracellular environment causes IgG release from FcRn. Any pinocytosed or endocytosed proteins, including IgG, that are not rescued in this manner are efficiently trafficked to the lysosomes for degradation (1–3).

Epithelial monolayers lining the mucosal surfaces polarize into two separate plasma membrane domains, the apical and basolateral, which are separated by intercellular tight junctions at the apical poles. The vast mucosal surfaces represent major sites of potential attack by invading pathogens. Receptor-mediated endocytosis of viruses and postendocytic membrane fusion has long been accepted as a cell entry mechanism for many viruses (7). For enveloped viruses, fusion of the viral lipid bilayer with the membrane of an acidic endosome is generally catalyzed by a "fusion protein" on the viral surface (8). Influenza A virus infection begins with the interaction of virions with cell surface sialic acid residues (9) primarily mediated by hemagglutinin (HA). After binding, virions are internalized through endocytic pathways (10). The acidic pH within the endosomes induces a conformational change in the viral HA, which in turn triggers fusion between the viral envelope and the endosomal membranes. Subsequently, the viral matrix and viral ribonucleoprotein (vRNP) are ejected into the cytoplasm and the vRNP is actively imported into the nucleus. Viral proteins produced in the cytoplasm assemble with replicated viral RNA and bud from the cell membrane.

Mucosal antibody provides a primary line of defense against pathogen invasion (11). Although studies have shown that FcRn is responsible for shuttling IgG (12–14), the exact role of FcRn-mediated IgG transport in mucosal protection remains elusive. Intriguingly, acidic endosomes appear to be the primary compartment in which FcRn resides and functions, and endocytosed virions initiate fusion of their envelopes within these compartments. Therefore, the endosome would be an ideal site for the transcytosed IgG to meet internalized virions within polarized epithelial cells. This led us to speculate that FcRn traffics extracellular virus-specific IgG to the endosomes of epithelial cells, where it prevents virus replication. To investigate this hypothesis, we used an mAb, Y8-10C2 (Y8), that binds to the monomeric but not trimeric form of influenza HA, corresponding to conformational changes induced by acidic pH (15). Our data show that FcRn-mediated transport of Y8 mAb results in the neutralization of viral infection in the epithelial endosomes by blocking viral envelope fusion with endosomal membranes, sub-

Author contributions: Y.B., L.Y., and X.Z. designed research; Y.B., L.Y., D.B.T., H.S., and D.Z. performed research; P.J.B. and D.C.R. contributed new reagents/analytic tools; Y.B., L.Y., P.J.B., D.C.R., and X.Z. analyzed data; and D.B.T., P.J.B., D.C.R., and X.Z. wrote the paper.

The authors declare no conflict of interest.

This article is a PNAS Direct Submission.

[1]Y.B. and L.Y. contributed equally to this work.

[2]To whom correspondence may be addressed E-mail: bjorkman@caltech.edu or xzhu1@umd.edu.

This article contains supporting information online at www.pnas.org/lookup/suppl/doi:10.1073/pnas.1115348108/-/DCSupplemental.

sequently resulting in the arrest of viral replication. These data suggest that FcRn/IgG plays a unique role in the intracellular defense, in addition to the role it plays extracellularly. This finding may have implications for the design of vaccines or antibody-based therapies.

Results

FcRn-Mediated IgG Neutralization of Influenza Virus. Transcytosis of the FcRn-IgG complex can be faithfully recapitulated in polarized Madin–Darby canine kidney (MDCK) cells stably transfected with rat FcRn and β2m (MDCK-FcRn) (5). Additionally, MDCK is a classic model cell line for replicating influenza virus. Y8 mAb can only detect PR8 HA in conformational forms induced by an acidic pH (Fig. S1). We thus selected MDCK-FcRn as a cell-based model system to test the hypothesis. Y8 mAb or an irrelevant IgG was added to the basolateral chamber of MDCK-FcRn to initiate transcytosis (Fig. S2). Subsequently, PR8 virus was added to the apical side to initiate infection. Viral yields were measured in the apical medium 24 h later by a 50% tissue culture infective dose ($TCID_{50}$) assay. The results showed that mAb Y8 reduced the yield of PR8 virus approximately 100-fold, but not in an MDCK-vector or IgG control monolayer (Fig. 1*A*). The extent of viral replication was further assessed by examining the expression of the influenza nucleoprotein (NP) gene. FcRn-mediated transcytosis of Y8 IgG, but not control IgG, significantly reduced the expression level of NP gene (Fig. S3). These data further suggest that the intracellular inhibition of virus replication is dependent on the transepithelial flux of IgG.

To further test whether the intracellular neutralization of influenza virus by Y8 mAb in MDCK-FcRn cells was dependent on FcRn-mediated IgG transcytosis, we performed two experiments. First, we used MDCK cells expressing a chimeric FcRn and GFP, which is unable to transcytose IgG (5), and we verified this result (Fig. S4*A*). Y8 mAb added to the basolateral chamber of MDCK-FcRn-GFP monolayers did not significantly reduce virus titers in comparison with those of control IgG-treated cells (Fig. 1*B*). In contrast, MDCK-FcRn cells produced significantly fewer viral progeny when incubated basolaterally with Y8 mAb. Second, the virus titers in MDCK-FcRn/IgG cells that were pretreated with nocodazole reached comparable levels to those observed in untreated MDCK-vector cells (Fig. S4 *B* and *C*). We conclude that the intracellular neutralization of virus by Y8 mAb is dependent on FcRn-mediated IgG transport by polarized epithelial cells.

Colocalization of FcRn, Virus, and IgG in Endosomal Compartment. FcRn binding to IgG and Y8 mAb binding to PR8 virions both occur only at acidic pH. Acidic conditions also cause fusion between the endosomal membrane and the viral envelope. We speculated that Y8 mAb transported into these endosomal compartments by FcRn might interact with virus particles endocytosed from apical epithelial surfaces. To test this possibility, we performed confocal analysis of confluent MDCK-FcRn cells that were incubated with Y8 mAb and further infected with biotin-labeled PR8 virus. As expected, the staining appeared in punctuate and vesicular patterns (Fig. S5). Pair-wise colocalization of PR8 virus or FcRn with Y8 mAb showed significant colocalization (yellow, Fig. S5, *Upper*) in all cases. Furthermore, both Y8 mAb (blue, Fig. S5) and PR8 virus (red, Fig. S5) colocalized with the early endosomal marker EEA1 (green, Fig. S5) in three-color confocal experiments (white, Fig. S5, *Lower*). Most importantly, the colocalization results were confirmed by staining MDCK-FcRn cells that were inoculated basolaterally with Y8 mAb and apically infected with PR8 (Fig. 2). A Z-stack reconstructed view showed that the colocalization only occurred on the apical sides, suggesting Y8 IgG had been transported from the basolateral to apical domain.

Y8 mAb Neutralizes Viral Replication by Blocking Trafficking of Influenza vRNPs to the Nucleus. When influenza particles are endocytosed into endosomes, the acidic pH triggers fusion between the viral envelope and the endosomal membranes and release of vRNPs into the cytoplasm, with subsequent travel to the nucleus to initiate replication. If the Y8 mAb acts by preventing viral envelope fusion with the endosomal membrane, it should prevent the trafficking of vRNPs to the nucleus. To test this, infected cells were stained with mAb anti-EEA1, an early endosome marker, or anti-NP protein to visualize vRNP trafficking to the nucleus. We were able to detect PR8 NP proteins (red, Fig. 3*A*) in the nucleus in control IgG-treated cells 1 h after infection (Fig. 3*A*), but not in the Y8 mAb-treated cells (Fig. 3*A*). Interestingly, the overall density of NP staining was significantly increased in control IgG-treated cells (Fig. 3*A*). One possible explanation is that NP was made rapidly in cells that

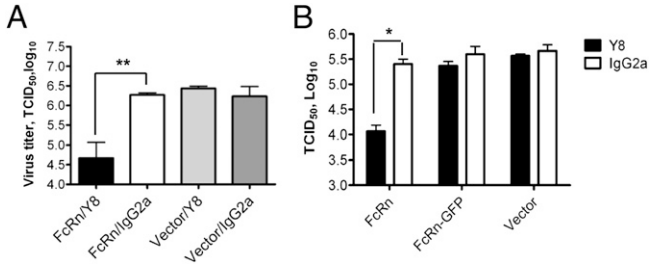

Fig. 1. Neutralization of influenza PR8 virus in MDCK-FcRn cells by Y8 mAb. Cells (1×10^5/well) were grown in a 0.4-μm transwell insert and allowed to polarize. (*A*) Neutralization of PR8 virus by Y8 mAb transcytosis. Y8 mAb or IgG2a isotype (400 μg/mL) was added to the basolateral chamber for 2 h at 37 °C; subsequently, PR8 virus (100 pfu/cell) was added to the apical chamber for 1.5 h at 4 °C, then switched to 37 °C for 45 min. Cells in both chambers were completely washed of residual IgG to remove adherent virus particles. Monolayers were then incubated for an additional 24 h at 37 °C. The amount of PR8 virus in the apical medium was analyzed by $TCID_{50}$ assay. (*B*) Neutralization of PR8 virus by Y8 mAb is dependent on IgG transcytosis. Y8 mAb (400 μg/mL) was added to the basolateral chamber of MDCK-FcRn, MDCK-FcRn-GFP, or control cells for 2 h at 37 °C. PR8 virus was subsequently added to the apical side for 1.5 h at 4 °C, and then cells were switched to 37 °C for another 45 min to allow for infection. The remaining procedures were performed as in *A*. $*P < 0.05$ and $**P < 0.01$.

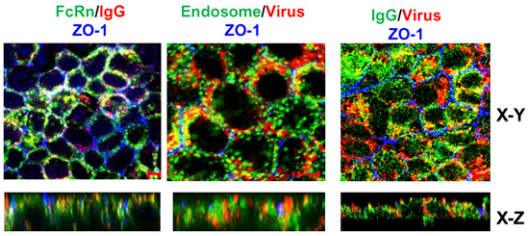

Fig. 2. Intracellular colocalizations of Y8 mAb, FcRn, PR8 virus, and endosome. Colocalization of FcRn, EEA1, IgG, and PR8 virus in MDCK-FcRn cells. Cells were grown in 0.4-μm inserts and allowed to polarize. Y8 mAb (400 μg/mL) was added to the basolateral side for 2 h at 37 °C, and subsequently, biotin-PR8 virus (100 pfu/cell) was added to the apical side for 1.5 h at 4 °C. Cells were then incubated for 45 min at 37 °C and thoroughly washed to remove the residual IgG. Cells were fixed and permeabilized. MDCK-FcRn cells were incubated with mouse anti-FcRn (1G3 mAb) or mAb anti-EEA-1 (5 μg/mL) or ZO-1 (5 μg/mL), respectively, followed by Alexa Fluor 488- or Alexa Fluor 555-conjugated IgG of the corresponding species. XY sections are taken at the level of the ZO-1 staining, and the XZ sections are shown (*Lower*). The ZO-1 staining (blue) indicates the tight junctions at the apical pole of the MDCK-FcRn cells. Colocalization of red and green signals creates a yellow-orange color. (Scale bars: 5 μm.)

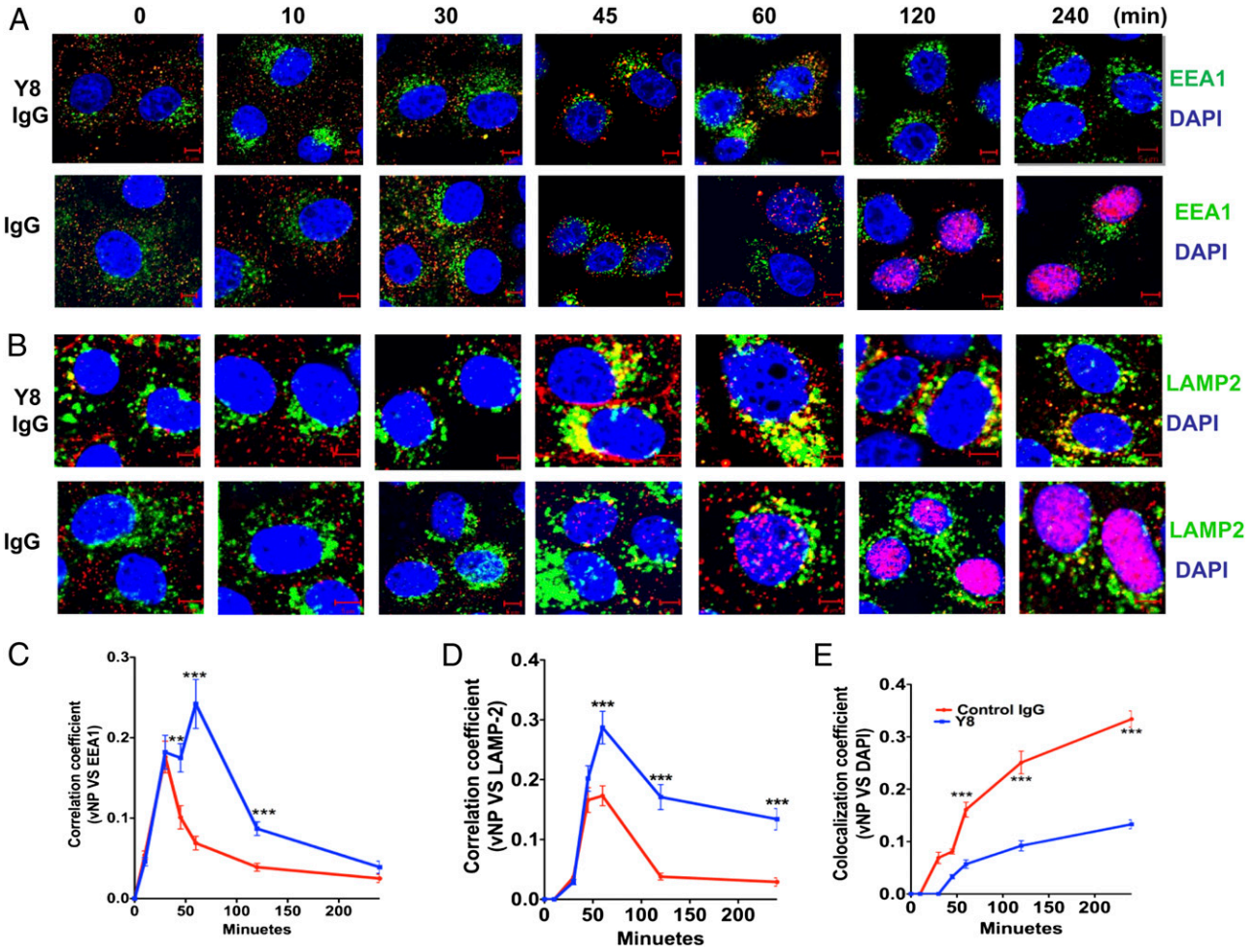

Fig. 3. Y8 mAb blocks the entry of PR8 ribonucleoprotein into the nucleus following infection. MDCK-FcRn cells were incubated with Y8 mAb or control IgG2a (400 μg/mL) for 2 h. Cells were then infected with PR8 virus at a multiplicity of infection of 100 pfu/cell at 4 °C for 1.5 h to allow virus attachment. Subsequently, infected cells were shifted to 37 °C to allow virus infection at indicated time points. Cells were fixed, permeabilized, and blocked before staining with mAb anti–EEA-1 (5 μg/mL) (*A*) or anti–LAMP-2 (5 μg/mL) (*B*) followed by Alexa Fluor 488- or Alexa Fluor 555-conjugated IgG. NP proteins were stained red by HB-65 mAb for the appearance of PR8 at indicated time. The nucleus is stained with DAPI (*blue*). (Scale bar: 5 μm.) Pearson colocalization coefficient was calculated to represent the colocalization between NP protein and EEA1 (*C*), LAMP-2 (*D*), and DAP1 (*E*) in PR8-infected MDCK-FcRn cells treated with Y8 mAb or control IgG at different time points following infection. Ten cells were analyzed from at least three different optical regions at each time point by using LSM5 image examiner software (Zeiss).$^{**}P < 0.01$ and $^{***}P < 0.001$.

were infected with this amount of virions, so the observed staining may represent newly synthesized NP. However, in at least one previous study, newly synthesized NP was not detected until 4 h after infection, with the maximum synthesis occurring at approximately 8 to 9 h (16).

To further investigate the fate of virus particles, anti–lysosome-associated membrane glycoprotein-2 (LAMP-2), a lysosomal marker, and anti-NP mAbs were used to follow virion trafficking to nuclear or lysosomal sites. Transport of the virus particles to the lysosomes was negligible in control IgG-treated MDCK-FcRn cells during the incubation periods indicated (Fig. 3*B*). However, the colocalization (yellow, Fig. 3*B*) of LAMP-2 and virus particles became more prominent at 45 min in Y8 mAb-treated cells, suggesting that this antibody promotes the trafficking of virus particles into the lysosomes (Fig. 3*B*). Pearson correlation coefficient analysis indicated a significant colocalization of viral NP protein with endosomal (Fig. 3*C*), lysosomal (Fig. 3*D*), and nucleus markers (Fig. 3*E*). Taken together, these data strongly suggest that the Y8 mAb prevents influenza virus entry into the nucleus, possibly by retaining the virus in endocytic compartments and by inhibiting the fusion of virus envelope and endosomal membranes, ultimately resulting in the delivery of these particles to lysosomes for degradation.

Prophylactic Efficacy of Y8 mAb Against PR8 Influenza Challenge in Vivo. Given FcRn expressed in the airway and mediated IgG transport across the airway mucosal barrier (Figs. S6 and S7), it was of interest to know whether passive transfer of Y8 mAb could confer protection from PR8 infection in mice. Groups of five WT and five FcRn-KO mice each received 100 μg of purified Y8 mAb via an intraperitoneal injection. Control groups of WT mice received isotype-matched IgG or sterile PBS solution. All mice were intranasally challenged 4 h later with a lethal dose (500 pfu) of PR8 virus. Because the serum half-life of IgG is greatly reduced in FcRn-KO mice (17, 18), we injected the FcRn KO mice daily with 25–57.5 μg of Y8 mAb to compensate for IgG degradation. This supplementation strategy was first confirmed by injecting biotin-labeled IgG in a pilot experiment. In this way, the concentrations of Y8 mAb were expected to be similar between WT and FcRn-KO mice. Survival rates (Fig. 4*A*) and body weight losses (Fig. 4*B*) were then monitored. All WT animals that received Y8 mAb survived, whereas only 40% of the

animals in the FcRn-KO group survived ($P < 0.05$). The majority of animals that received irrelevant IgG or PBS solution died of infection within 6 d after challenge. Therefore, the administration of Y8 mAb in the WT mice was clearly associated with a survival benefit compared with control animals. Although the FcRn-KO mice receiving the Y8 mAb showed a trend toward increased survival, the increase was not significantly different from control animals. In addition, WT animals treated with Y8 mAb did not significantly lose body weight, whereas the mean weight loss in the control group was approximately 30% by the time the mice died or were euthanized ($P < 0.01$). FcRn-KO mice that received Y8 mAb showed similar decreases in body weight as the control animals, with a 25% mean weight loss (Fig. 4*B*). In addition, all animals were assessed for viral load in the lungs at day 1 (Fig. 4*C*) or day 5 (Fig. 4*D*) after infection, after necropsy. The levels of virus in the lungs of WT mice, but not FcRn-KO mice treated with Y8 mAb, were 2.5 to 3 $\log_{10}$ $TCID_{50}$ lower than that in the control group (both $P < 0.01$).

Pathological results were in accordance with the findings described earlier. No lesions were present in the lungs of mock-infected mice (Fig. 5*A*, normal control). In H36-4 (Fig. S1 and *SI Results*) mAb-treated animals, the loss of infectivity attributable to the combined inhibition of attachment and inhibition of fusion was sufficient to account for the extent of neutralization caused by relatively low concentrations of H36-4 mAb. WT animals that received Y8 mAb showed much less pulmonary pathology, such as edema or hemorrhagic appearance, or showed such lesions at a lower grade of severity, compared with control antibody- or PBS solution-treated animals (Fig. 5*A*). Examination of lungs in mice that received Y8 mAb on day 6 or 8 after infection revealed that mice did not develop apparent inflammatory changes, although a slightly increased lymphocytic perivascular cuffing was observed (Fig. 5*B*, images 5 and 7). Examination of lungs in mice that received H36-4 mAb on day 6 or 8 after infection revealed a similar level of resolution (Fig. 5*B*, image 3). In contrast, FcRn KO mice that received Y8 developed peribronchiolar pneumonia that increased in severity, and a necrotizing bronchitis and bronchiolitis also appeared at this time point (Fig. 5*B*, images 6 and 8). Mice that received PBS solution and irrelevant IgG had continued peribronchiolar pneumonia and necrotizing bronchiolitis at day 6 after infection; the pneumonia was more widespread (Fig. 5*B*, images 2 and 4). The unprotected animals all died at day 6 to 7 after infection. Overall, these findings show that prophylactically administered Y8 mAb confers protection against lethal PR8 challenge, prevents mortality and viral replication, and reduces pulmonary pathology in an FcRn-dependent manner.

Discussion

IgG is the predominant Ig isotype present in the lungs (19). In the context of influenza virus, passive immunization by vertical acquisition (20) or passive transfer (21, 22) demonstrates a clear role for virus-specific murine or humanized IgG antibodies in prophylaxis and therapy in both animal models as well as in infant humans. However, the precise cellular mechanisms by which these antibodies protect against viral infection and/or propagation remain elusive. Although the direct neutralization of viral particles is believed to be the primary function of antibodies in antiviral immunity, IgG is also efficient at fixing complement and binding to Fc receptors on cells (11, 23). Indeed, "nonneutralizing" antibody-dependent cellular cytotoxicity has been demonstrated in viral infection (24). However, these functions all require extracellular interactions, which should not occur between Y8 mAb and HA because this antibody is unable to bind HA at neutral pH. In this study, we show that anti-influenza IgG antibodies, traditionally considered to be nonneutralizing IgG, are in fact capable of blocking viral infection in polarized epithelial cells via a mechanism that is dependent on FcRn-mediated transport of IgG.

To directly determine whether Y8 interferes within influenza infection, the intracellular neutralizing potential of Y8 mAb was evaluated by mimicking the mucosal epithelial barrier in vitro. Y8, but not control IgG, significantly reduced PR8 viral replication, suggesting that the blocking of viral replication by Y8 is

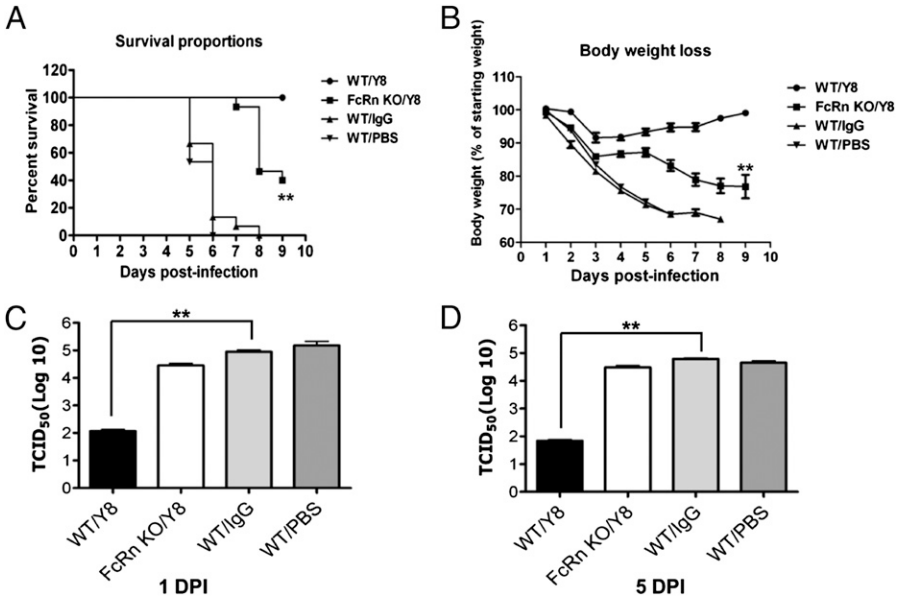

Fig. 4. PR8 HA-specific Y8 mAb protected mice from virus infection. (*A* and *B*) Severity of infection in mice challenged with PR8 virus. Groups of five WT and FcRn-KO mice were intraperitoneally injected with 100 μg Y8 mAb or control IgG. One group of five mice was mock-injected with PBS solution. Four hours later, mice were intranasally challenged with 500 pfu of PR8 virus. The mice were monitored for 10 d. FcRn-KO mice were injected daily with 25–57.5 μg Y8 or control IgG to compensate for IgG catabolism. (*A*) Survival rate was assessed by recording whether the mice died from the infection. Percentage of mice protected on the indicated days was calculated as the number of mice surviving divided by the number of mice in each group and averaged over three similar experiments ($n = 15$). The mice were also weighed daily to monitor illness, as defined by percent weight loss (*B*). For virus titration, lungs were harvested at day 1 (*C*) or day 5 (*D*) after infection and homogenized. The amount of PR8 virus in the supernatant was analyzed by $TCID_{50}$. Data shown are the means of three independent experiments, with five mice per group (**$P < 0.01$).

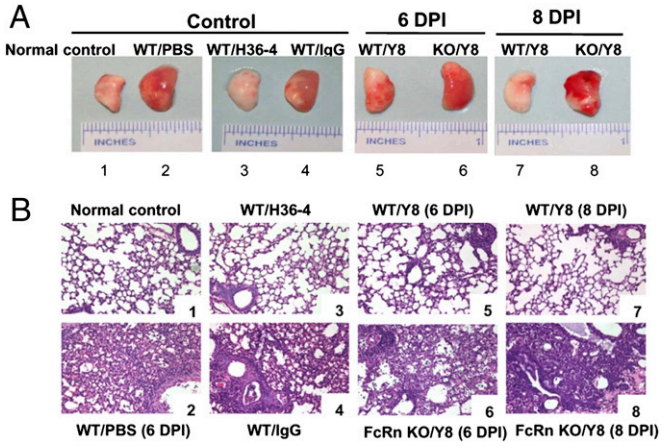

Fig. 5. Lung pathologic findings following PR8 virus challenge. (*A*) Gross pathology of the lung. The lung exhibited edema and a hemorrhagic appearance in the absence of Y8 mAb inoculation or in FcRn-KO mice inoculated with Y8 mAb. H36-4 mAb was used as a positive control. (*B*) Histopathology in the lung of PR8-infected mice at 6 or 8 d. Inflammation was most severe in infected mice on day 6. After infection with PR8, WT mice treated with Y8 (WT/Y8) or H36 mAb (WT/H36) exhibited few focal areas of epithelial necrosis and peribronchial hemorrhage; however, the WT mice treated with PBS solution or irrelevant IgG, or FcRn-KO mice inoculated with Y8 mAb, showed severe peribronchial inflammation and bronchiolar necrosis with necrotic epithelial cells present in the lumen, and submucosal edema and vascular congestion. A mixed infiltration of inflammatory cells was present throughout at day 6 after infection. All unprotected animals died between days 6 and 7 after infections. Positive control infected mice had similar bronchiolar necrosis as control IgG-inoculated mice. Mock-infected mice had no lesions.

dependent on transepithelial transcytosis of IgG by FcRn. Furthermore, Y8 colocalized with virions and FcRn inside endosomes, consistent with previous studies of the intracellular colocalization of these proteins. Most importantly, Y8 mAb did not bind the PR8 virus at neutral pH, excluding the possibility that the Y8 neutralized virus in an extracellular environment. Therefore, the Y8 mAb most likely interrupted viral replication during its encounter with viral particles in acidic endosomal compartments. We further examined the capacity of Y8 mAb to inhibit PR8 virus replication and reduce lung inflammation when Y8 mAb was administered to WT and FcRn-KO mice. Y8 mAb in WT mice provided strong protection from lethality, prevented weight loss, provided a significant reduction in pulmonary virus titers, and largely reduced virus-induced inflammation in the lungs. However, it should be noted that Y8 conferred some (albeit significantly less) protection from postinfection lethality and weight loss in FcRn-KO mice. This FcRn-independent effect may be a result of fluid-phase uptake of the Y8 mAb into cells and endosomal entry in vivo. Overall, our results support a mechanism in which FcRn mediates the intracellular transport of anti-influenza IgG antibodies for endosomal neutralization sites in polarized epithelial cells.

What are the critical steps at which the Y8 mAb interferes with the viral life cycle during its trafficking by FcRn? An acidic pH is critical for FcRn binding to Y8 and for Y8 to interact with HA. Y8 mAb was shown to bind to internalized virus but not to virus absorbed to the cell surface (Fig. S1). This finding is consistent with the fact that Y8 can bind to HA only following conformational changes caused by a low pH such as those that occur inside endosomes (15, 25). Y8 might therefore sterically block an interaction between the endosomal membrane and a region of the influenza HA responsible for fusion. As such, FcRn may organize IgG in the endosome in an orientation that facilitates the interaction with viral HA. Alternatively, FcRn might simply increase the endosomal concentrations of IgG to levels that more effectively block viral fusion.

FcRn-mediated transport of IgG can be divided into several steps: IgG pinocytosis from the basolateral membrane to basolateral recycling endosomes, translocation from basolateral early endosomes to apical recycling endosomes (ARE), and finally, IgG recycling between the ARE and the apical plasma membrane (1, 2). Therefore, transcytosis should result in the accumulation of FcRn/Y8 mAb in the ARE. Intracellular neutralization is likely to result from the fusion of transcytotic vesicles containing Y8 mAb with vesicles containing endocytosed virions, suggesting that Y8 mAb blocks acid-induced fusion of the viral and endosome membranes required for vRNP entry into the cytoplasm and nucleus. In the present study, inhibition of this fusion process was strongly suggested by the fact that NP antigen from Y8 IgG-neutralized virus, unlike that of nonneutralized virus, did not accumulate in the nucleus; instead, it was enriched in the lysosomes. Live cell imaging analyses of endothelial cells provides strong evidence that FcRn can traffic its ligands to the lysosomes (26). FcγRI and FcγRIII engagement by IgG–bacteria immune complexes target intracellular bacteria to lysosomes in macrophages for degradation by a process strictly dependent on protein kinases involved in FcR intracellular signaling (27). Although these mechanisms are found in endothelial cells or macrophages, it is interesting to determine whether similar intracellular signaling and trafficking pathways operate in polarized epithelial cells to target antibody-coated viruses to lysosomes. Furthermore, although we used a highly pH-dependent mAb to demonstrate intracellular neutralization, a pH-independent IgG that binds HA at a location that prevents a conformational change required for fusion might function in both extracellular neutralization and, upon encountering virus within endosomes, intracellular neutralization.

It is intriguing that Y8 mAb binds to the globular but not the fusion domain of the stalk region of influenza HA (15). It has been shown that membrane fusion mediated by the influenza HA requires the concerted action of at least HA trimers (28). By binding to low pH-induced monomeric HA molecules, Y8 mAb might prevent a structural transition of HA required for fusion, as shown in a previous study (29). Thus, Y8 mAb may neutralize intracellularly because it blocks fusion and egress from endosomes, resulting in the transport of virions to the lysosome for destruction. It is possible that other IgG antibodies with a broader spectrum of action or directed against the HA stalk regions containing the fusion domain might work similarly, or even more effectively, by FcRn-dependent intracellular neutralization mechanisms at the mucosal surface. It would be interesting to know if intracellular neutralization would be effective against a broad spectrum of influenza subtypes and antigenic drift variants as a result of the possible conservation of the antibody recognition site in the fusion domain. For example, antibodies can broadly recognize a highly conserved influenza virus epitope in the stalk regions of influenza HA (30, 31); a vaccine based on the conserved HA stalk domain provided full protection against death and partial protection against disease following lethal viral challenge (32). Thus, heterotypic immunity probably involves several distinct immunological pathways, and this study illustrates that FcRn-mediated IgG transcytosis contributes to an intracellular neutralization mechanism.

The current paradigm for antibody-mediated mucosal immunity is that polymeric IgA receptor-mediated transcytosis of dimeric IgA releases secretory IgA into mucosal secretions by proteolytic cleavage. This transport process makes it possible for secretory IgA to block the binding of viruses to their entry receptors on the cell surface and to neutralize intracellular viruses (33–35). In this study, FcRn-mediated IgG transcytosis provides a mechanism for eliminating intracellular pathogens

without destroying epithelial integrity (Fig. S8). This protective mechanism is determined by intracellular interactions between IgG and viral proteins enabled by the FcRn-mediated transport of IgG, by the specificity of the IgG for a particular viral component, and by the life cycle of the virus within mucosal epithelial cells. Similar intracellular neutralization mechanisms might be applicable for HIV (36) as well as bacteria (37). Recently, a cytosolic IgG receptor, tripartite motif-containing 21, bound and targeted incoming antibody–virus complexes to the proteasome via its E3 ubiquitin ligase activity (38). Our finding that FcRn efficiently delivers IgG to intracellular vesicles may provide an endosomal route for access to this cytosolic receptor. A greater understanding of the mechanisms by which strongly inhibitory antibodies act intracellularly may influence the design of novel vaccines (39) or antibody-based therapies.

Methods

All cells were grown in DMEM complete medium in 5% CO_2 at 37 °C. Influenza A virus (strain A/Puerto Rico/8/1934 H1N1) was grown in 10- to 11-d-old embryonated chicken eggs. All PR8 virus-specific mAbs and staining antibodies were purchased. The FcRn-KO mice in a C57BL/6 background were from Jackson Laboratory. All animal studies were approved by the institutional animal care and use committee at the University of Maryland. *SI Methods* provides further details.

ACKNOWLEDGMENTS. We thank Geoffrey J. Letchworth for critical reading of the manuscript, Peter Palese for the influenza PR8 strain, and Keith Mostov for the Madin–Darby canine kidney type II cell line; Neil Simister for helpful discussions of mouse IgG catabolism; and Senthilkumar Palaniyandi, Rongyu Zeng, Xindong Liu, Zili Li, and Yunsheng Wang for technical help. This work was supported in part by National Institutes of Health Grants AI65892 (to X.Z.), AI67965 (to X.Z.), AI73139 (to X.Z.), DK56597 (to D.C.R.), and R37 AI041239-06A1 (to P.J.B.).

1. Ward ES, Ober RJ (2009) Chapter 4: Multitasking by exploitation of intracellular transport functions the many faces of FcRn. *Adv Immunol* 103:77–115.
2. Roopenian DC, Akilesh S (2007) FcRn: The neonatal Fc receptor comes of age. *Nat Rev Immunol* 7:715–725.
3. Baker K, et al. (2009) Immune and non-immune functions of the (not so) neonatal Fc receptor, FcRn. *Semin Immunopathol* 31:223–236.
4. Raghavan M, Bonagura VR, Morrison SL, Bjorkman PJ (1995) Analysis of the pH dependence of the neonatal Fc receptor/immunoglobulin G interaction using antibody and receptor variants. *Biochemistry* 34:14649–14657.
5. Tesar DB, Tiangco NE, Bjorkman PJ (2006) Ligand valency affects transcytosis, recycling and intracellular trafficking mediated by the neonatal Fc receptor. *Traffic* 7: 1127–1142.
6. Ober RJ, Martinez C, Vaccaro C, Zhou J, Ward ES (2004) Visualizing the site and dynamics of IgG salvage by the MHC class I-related receptor, FcRn. *J Immunol* 172: 2021–2029.
7. Tucker SP, Compans RW (1993) Virus infection of polarized epithelial cells. *Adv Virus Res* 42:187–247.
8. White JM, Wilson IA (1987) Anti-peptide antibodies detect steps in a protein conformational change: Low-pH activation of the influenza virus hemagglutinin. *J Cell Biol* 105:2887–2896.
9. Nicholls JM, Chan RW, Russell RJ, Air GM, Peiris JS (2008) Evolving complexities of influenza virus and its receptors. *Trends Microbiol* 16(4):149–157.
10. Rust MJ, Lakadamyali M, Zhang F, Zhuang X (2004) Assembly of endocytic machinery around individual influenza viruses during viral entry. *Nat Struct Mol Biol* 11:567–573.
11. Corthesy B, Kraehenbuhl J-P (1999) Antibody-mediated protection of mucosal surfaces. *Curr Top Microbiol Immunol* 236:93–111.
12. Spiekermann GM, et al. (2002) Receptor-mediated immunoglobulin G transport across mucosal barriers in adult life: Functional expression of FcRn in the mammalian lung. *J Exp Med* 196:303–310.
13. Yoshida M, et al. (2006) Neonatal Fc receptor for IgG regulates mucosal immune responses to luminal bacteria. *J Clin Invest* 116:2142–2151.
14. Li Z, et al. (2011) Transfer of IgG in the female genital tract by MHC class I-related neonatal Fc receptor (FcRn) confers protective immunity to vaginal infection. *Proc Natl Acad Sci USA* 108:4388–4393.
15. Yewdell JW, Gerhard W, Bächi T (1983) Monoclonal anti-hemagglutinin antibodies detect irreversible antigenic alterations that coincide with the acid activation of influenza virus A/PR/834-mediated hemolysis. *J Virol* 48:239–248.
16. Momose F, Kikuchi Y, Komase K, Morikawa Y (2007) Visualization of microtubule-mediated transport of influenza viral progeny ribonucleoprotein. *Microbes Infect* 9: 1422–1433.
17. Israel EJ, Wilsker DF, Hayes KC, Schoenfeld D, Simister NE (1996) Increased clearance of IgG in mice that lack beta 2-microglobulin: Possible protective role of FcRn. *Immunology* 89:573–578.
18. Roopenian DC, et al. (2003) The MHC class I-like IgG receptor controls perinatal IgG transport, IgG homeostasis, and fate of IgG-Fc-coupled drugs. *J Immunol* 170: 3528–3533.
19. Reynolds HY (1987) Identification and rôle of immunoglobulins in respiratory secretions. *Eur J Respir Dis Suppl* 153:103–116.
20. Reuman PD, Paganini CM, Ayoub EM, Small PA, Jr. (1983) Maternal-infant transfer of influenza-specific immunity in the mouse. *J Immunol* 130:932–936.
21. Renegar KB, Small PA, Jr., Boykins LG, Wright PF (2004) Role of IgA versus IgG in the control of influenza viral infection in the murine respiratory tract. *J Immunol* 173: 1978–1986.
22. Simmons CP, et al. (2007) Prophylactic and therapeutic efficacy of human monoclonal antibodies against H5N1 influenza. *PLoS Med* 4(5):e178.
23. Forthal DN, Moog C (2009) Fc receptor-mediated antiviral antibodies. *Curr Opin HIV AIDS* 4:388–393.
24. Florese RH, et al. (2006) Evaluation of passively transferred, nonneutralizing antibody-dependent cellular cytotoxicity-mediating IgG in protection of neonatal rhesus macaques against oral SIVmac251 challenge. *J Immunol* 177:4028–4036.
25. Bächi T, Gerhard W, Yewdell JW (1985) Monoclonal antibodies detect different forms of influenza virus hemagglutinin during viral penetration and biosynthesis. *J Virol* 55: 307–313.
26. Gan Z, Ram S, Vaccaro C, Ober RJ, Ward ES (2009) Analyses of the recycling receptor, FcRn, in live cells reveal novel pathways for lysosomal delivery. *Traffic* 10:600–614.
27. Joller N, et al. (2010) Antibodies protect against intracellular bacteria by Fc receptor-mediated lysosomal targeting. *Proc Natl Acad Sci USA* 107:20441–20446.
28. Danieli T, Pelletier SL, Henis YI, White JM (1996) Membrane fusion mediated by the influenza virus hemagglutinin requires the concerted action of at least three hemagglutinin trimers. *J Cell Biol* 133:559–569.
29. Barbey-Martin C, et al. (2002) An antibody that prevents the hemagglutinin low pH fusogenic transition. *Virology* 294(1):70–74.
30. Ekiert DC, et al. (2009) Antibody recognition of a highly conserved influenza virus epitope. *Science* 324:246–251.
31. Sui J, et al. (2009) Structural and functional bases for broad-spectrum neutralization of avian and human influenza A viruses. *Nat Struct Mol Biol* 16:265–273.
32. Steel J, et al. (2010) Influenza virus vaccine based on the conserved hemagglutinin stalk domain. *mBio* 1:pii:e00018-10.
33. Kaetzel CS, Robinson JK, Chintalacharuvu KR, Vaerman JP, Lamm ME (1991) The polymeric immunoglobulin receptor (secretory component) mediates transport of immune complexes across epithelial cells: A local defense function for IgA. *Proc Natl Acad Sci USA* 88:8796–8800.
34. Mazanec MB, Kaetzel CS, Lamm ME, Fletcher D, Nedrud JG (1992) Intracellular neutralization of virus by immunoglobulin A antibodies. *Proc Natl Acad Sci USA* 89: 6901–6905.
35. Burns JW, Siadat-Pajouh M, Krishnaney AA, Greenberg HB (1996) Protective effect of rotavirus VP6-specific IgA monoclonal antibodies that lack neutralizing activity. *Science* 272(5258):104–107.
36. Bomsel M, et al. (1998) Intracellular neutralization of HIV transcytosis across tight epithelial barriers by anti-HIV envelope protein dIgA or IgM. *Immunity* 9:277–287.
37. Casadevall A (1998) Antibody-mediated protection against intracellular pathogens. *Trends Microbiol* 6(3):102–107.
38. Mallery DL, et al. (2010) Antibodies mediate intracellular immunity through tripartite motif-containing 21 (TRIM21). *Proc Natl Acad Sci USA* 107:19985–19990.
39. Ye L, Zeng R, Bai Y, Roopenian DC, Zhu X (2011) Efficient mucosal vaccination mediated by the neonatal Fc receptor. *Nat Biotechnol* 29(2):158–163.